IEICE TRANS. COMMUN., VOL.E95–B, NO.1 JANUARY 2012

INVITED PAPER *Special Section on Recent Progress in Antennas and Propagation in Conjunction with Main Topics of ISAP2010*

# Design of MIMO Antennas for Indoor Base Station and Mobile Terminal

**Hiroyuki ARAI**[†a)], ***Fellow and*** **Daisuke UCHIDA**[†], ***Student Member***

**SUMMARY** Two design parameters, SNR and correlation, are key factors for enhancing channel capacity in MIMO systems. Achieving high SNR and low correlation is desirable in antenna design. This paper discusses the relation between channel capacity and these two parameters, and presents simple formulas of this relation for propagation channels and antenna coupling of mobile terminals. According to these guidelines, indoor base station antennas are designed and examined using propagation measurements. We also present a suitable antenna design for mobile terminal antennas and based on a realistic propagation model, predicted the channel capacity of the antenna.

***key words:*** *MIMO, channel capacity, SNR, correlation, antenna*

## 1. Introduction

Multiple-input multiple-output (MIMO) systems are a key technology for the enhancement of communication capacity [1] and have been applied for WiMAX, LTE, and wireless LAN (IEEE 802.11n). Particularly in indoor environments, channel capacity has been evaluated in [2], [3]. For wireless LAN, the application of MIMO-orthogonal frequency division multiplexing (OFDM) was studied [4], [5] and several capacity enhancement schemes using antennas were proposed [6], [7]. Recently, femtocell networks have received considerable attention for facilitating very high-speed data transmission in indoor environments [8] and MIMO is expected as the key technology [9].

In the design of MIMO antennas with enhanced channel capacity in indoor environments, the main parameters are polarization, radiation pattern, and array configuration [10]–[12]. To this end, MIMO antennas with multi-polarization [13], [14], directive radiation patterns [15], and well-configured planar inverted-F antennas (PIFA) [16] have been proposed. Although directive radiation patterns have been confirmed to improve channel capacity in a few scenarios [17], [18], the suitable design in antenna radiation patterns is still left in order not to reduce mutual couplings but to enhance signal to noise ratio (SNR).

In this paper, two major parameters in MIMO systems, such as SNR and correlation, are evaluated with respect to enhancing channel capacity. To increase the SNR at reception points, we design two antennas: a patch antenna array and a dual polarization antenna consisting of a slot and dipole. These antennas are designed based on the results of ray-tracing simulations for indoor base stations (BS), which are typified by wireless LAN and femtocells. We also confirm the measured channel capacity of a BS equipped with the two antennas. The latter part of this paper is devoted to the design of mobile terminal (MT) antennas. A key design parameter, the correlation between antennas, is discussed using two simple dipoles as an example to show the relation with antenna efficiency and pattern distortion. We also demonstrate the enhancement of channel capacity, including the influence of phantom, for a suitable MT antenna. This paper concludes in Sect. 5.

Manuscript received April 11, 2011.
Manuscript revised August 15, 2011.

[†]The authors are with Graduate School of Engineering, Yokohama National University, Yokohama-shi, 240-8501 Japan.
a) E-mail: arai@ynu.ac.jp

DOI: 10.1587/transcom.E95.B.10

## 2. Channel Capacity

MIMO performance is characterized by channel capacity $C$, which is represented as [19],

$$C = \log_2\left(\det\left(\boldsymbol{I} + \frac{\rho}{N_t}\boldsymbol{H}_n\boldsymbol{H}_n^H\right)\right) \tag{1}$$

The above equation is transformed as follows [20].

$$C = N_r \log_2\left(\frac{\rho}{N_t}\right) + \log_2\left(\det\left(\boldsymbol{I}\cdot\frac{N_t}{\rho} + \boldsymbol{H}_n\boldsymbol{H}_n^H\right)\right) \tag{2}$$

$$\approx N_r \log_2\left(\frac{\rho}{N_t}\right) + \log_2\left(\det\left(\boldsymbol{H}_n\boldsymbol{H}_n^H\right)\right) = C_{SNR} + C_{COR} \tag{3}$$

where $\rho$ is the averaged SNR at each receiving antenna, $N_t$ and $N_r$ denote the number of the transmitting and receiving antennas, and $\mathbf{I}$ is a unit matrix. $\mathbf{H}_n$ is a normalized channel matrix and $\{\cdot\}^H$ represents a complex conjugate transpose. The approximation of Eq. (3) is satisfied when $N_r$ is greater than $N_t$, the channel is not ill-conditioned and $\rho$ is large. Equation (3) indicates that channel capacity contains elements depending on SNR ($C_{SNR}$) and correlation ($C_{COR}$).

Figure 1 shows the channel capacity as a function of SNR for four configurations of antenna elements, where

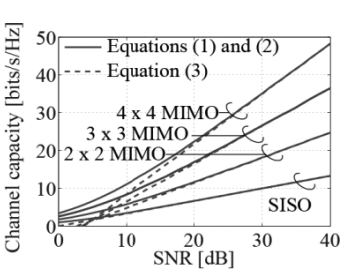


**Fig. 1** Channel capacity as a function of SNR.

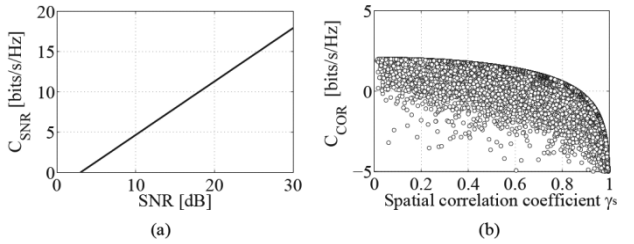


**Fig. 2** Performance of the components depending on (a) SNR and (b) correlation in $2 \times 2$ MIMO channel capacity.

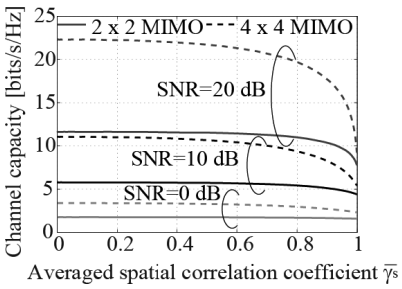


**Fig. 3** Channel capacity as a function of the averaged spatial correlation coefficient.

1,000 patterns of channel matrices are examined in each SNR and the average is used to evaluate the channel capacity. This result indicates that the channel capacity is increased with increase in SNR for antennas with a fixed element number. It should be noted that Eq. (3) is effective in high SNR regimes with a small number of elements.

To separately evaluate the contribution of SNR and correlation to channel capacity using Eq. (3), we focus on $2 \times 2$ MIMO systems. $C_{SNR}$ and $C_{COR}$ are shown in Fig. 2, where channel capacity is evaluated not based on $\det(\mathbf{H}_n \mathbf{H}_n^H)$, but rather the spatial correlation coefficient $\gamma_s$, which is defined by,

$$\gamma_s = \frac{R_{r,12}}{\sqrt{R_{r,11} R_{r,22}}} \tag{4}$$

where $R_{r,ii}$ is the components of $\mathbf{R}_r = \mathbf{H}\mathbf{H}^H$. Based on the modified Eq. (3), the relationship between SNR and channel capacity is clear, as shown in Fig. 2(a); a high SNR increases the channel capacity. $C_{COR}$ values are scattered below the upper bound in Fig. 2(b), since power distribution to the first and second eigenvalues is not optimized. The obtained upper bound curve indicates that low correlation provides high channel capacity, with the increasing ratio reaching saturation at $\gamma_s < 0.5$. Notably, the upper bound is given by the ideal propagation channel. Particularly in low SNR regime, the improvement rate of the channel capacity by the second term in Eq. (3) is high.

The above conclusions are based on the assumption of Rayleigh distribution in the propagation environment. We also examined the influence of SNR and correlation on channel capacity for Rician distribution. The averaged spatial correlation coefficient $\bar{\gamma}_s$ has a one-to-one correspondence with Rician factor$K$, and it is given by [21],

$$\bar{\gamma}_s = \frac{K}{K+1} \tag{5}$$

where $\bar{\gamma}_s$ is a monotone increasing function of $K$. Figure 3 shows the channel capacity in Eq. (1) as a function of $\bar{\gamma}_s$. Here, $\mathbf{H}_n$ is derived from the channel matrix $\mathbf{H}$, which is given by the following equation [22],

$$\boldsymbol{H} = \sqrt{\frac{K}{K+1}} \boldsymbol{H}_D + \sqrt{\frac{1}{K+1}} \boldsymbol{H}_{i.i.d} \tag{6}$$

$$\boldsymbol{H}_D = \begin{bmatrix} 1 & \cdots & 1 \\ \vdots & \ddots & \vdots \\ 1 & \cdots & 1 \end{bmatrix} \tag{7}$$

where $\mathbf{H}_{iid}$ is a matrix with complex Gaussian distribution. The channel matrices including $K$ are evaluated using the similar procedure as for Fig. 1. As shown in Fig. 3, the channel capacity increases in the low correlation regime, that is close to Rayleigh distribution. The increase of elements ($N_t$, $N_r$) and a high SNR are effective to enhance channel capacity under a Rician environment. However, the capacity is not increased for large $K$ regimes in MIMO systems.

## 3. Antenna Design for BS

Channel capacity in MIMO systems is increased by high SNR and low spatial correlation in the propagation channel. To satisfy this requirement, high gains with low correlated radiation patterns are required in BS antenna designs. BSs are often placed near the ceiling to realize a line-of-sight (LOS) environment for mobile terminals (MT). Here, we evaluate the design requirements for obtaining large channel capacity in a BS antenna for downlink transmissions and measure the channel capacity performance of the fabricated antenna. In this section, "correlation" indicates spatial correlation including the effect of the angular spread since the effects of the propagation channel are considered.

### 3.1 BS Placed in the Vicinity of Walls

To determine the suitable design guidelines for the MIMO antenna radiation patterns, parameter studies are conducted using ray-tracing propagation analysis based on the scenario presented in Fig. 4, where the variable $t$ denotes the aspect ratio of the room. In this scenario, the BS is placed near a wall, and the channel matrices are calculated in several MT positions. The environments between the BS and all MT positions are LOS without obstacles. The transmitting and noise powers are $-5$ dBm/ch and $-85$ dBm, respectively, and $2 \times 2$ MIMO communication is assumed. In [23], we clarified that the channel capacity of antennas adopting directive patterns was larger than that of antennas with omnidirectional patterns. Here, the radiation patterns of the BS are assumed to be pencil beam with an infinite front-to-back (FB) ratio [23], as shown in Fig. 4.

The half-power beam width (HPBW) ($\theta_h$) is fixed to 60°, and space-averaged channel capacities are then calculated for each angle between two beams ($\theta_s$). Figure 5

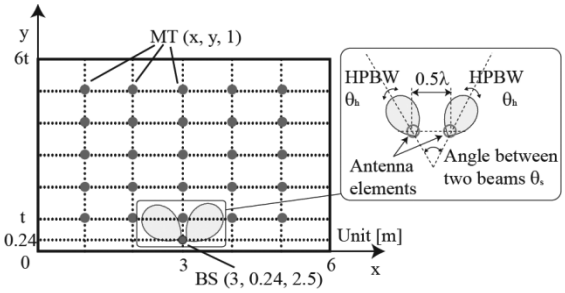


**Fig. 4** Analyzed room model and location of the BS and MT for determining suitable radiation patterns (overhead view). The room height is 2.7 m. $t$ denotes the aspect ratio of the room.

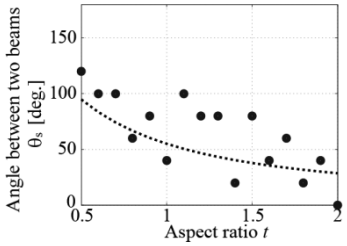


**Fig. 5** Angles between two beams leading to the maximum space-averaged channel capacity. ($\theta_h$ is fixed to 60°, and the dotted line indicates $\theta_s$ obtained when the main beams are pointed to the corner of the room.)

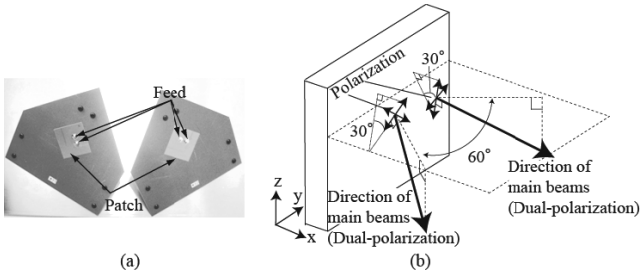


**Fig. 6** (a) Fabricated patch array. (b) Directions of the main beams.

shows the relationship between $\theta_s$ with the maximum space-averaged channel capacity and the aspect ratio. The distribution following the dotted line indicates that the main beam of the BS should be directed towards the room corners to increase the channel capacity. This improvement effect is not limited to $2\times2$ MIMO systems, as it was also confirmed for four streams. In [24], we demonstrated that a HPBW of 80° and tilt angle of 30° enhanced channel capacity. Here, we assumed $4\times4$ MIMO transmission by vertical and horizontal polarizations to reduce the correlation between antennas [25]. In addition, we showed that the capacity enhancement did not depend on the array arrangement of the MT [26].

The antenna based on the above design guidelines consists of a two-element patch antenna array with dual feeds, as illustrated in Fig. 6(a). Two beams with orthogonal polarizations are radiated from each patch antenna, and those are tilted downward, as shown in Fig. 6(b). Figure 7 shows the radiation patterns, and the HPBWs in the $yz$ and $zx$ planes are approximately 80° and 90°, respectively, and the antenna

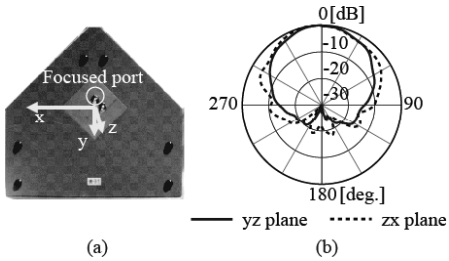


**Fig. 7** (a) Definition of the $x$, $y$, and $z$-axes in the BS patch antenna. (b) Radiation patterns in the $yz$ and $zx$ planes.

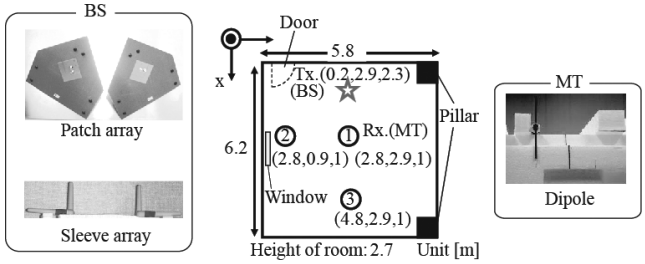


**Fig. 8** Measurement environment.

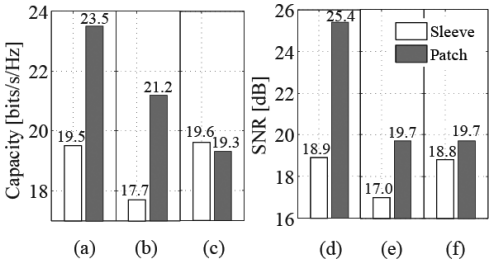


**Fig. 9** (a), (b), and (c) Channel capacities at MT positions 1, 2, and 3, respectively, for patch and sleeve antenna arrays. (d), (e), and (f) respective SNRs at the three positions.

gain is 7.0 dBi.

We measure the channel capacity of the BS adopting a patch array under the environment shown in Fig. 8. As a reference, a sleeve array is also used for a dual-polarization BS antenna, with the spacing between the vertical and horizontal oriented sleeves is equal to $1\lambda$. For MT antennas, a single dipole antenna is moved to evaluate sixteen channels' impulse responses by four channels because the measured environment is quasi-static and the time variation is almost negligible. Under this measurement condition, the element spacing between MT antennas is 0.5 $\lambda$. The BS antenna is placed on the ceiling near a wall and the channel matrices are measured at the three typical positions (1-3) for the MT, as shown in Fig. 8. At positions 1 and 3, the signals from the four beams of the BS are received at nearly the same level, and the SNR at position 1 is higher than that at position 3. At position 2, the signals from the left patch are dominant. In this measurement, the frequency is 2.45 GHz, and the measurement systems are described in detail in [25], [27].

Figure 9 shows the measured channel capacity and SNR for the three MT positions. At all positions, the SNRs

for the patch array-based antenna are higher than those for the reference antenna based on the sleeve array. The channel capacities are enhanced by the patch array, with improvements of 20% at positions 1 and 2. The channel capacity for the patch array is slightly smaller than that for the sleeve array at position 3. This is caused by degradation of the fourth eigenvalue, which is minimum eigenvalue, in the spatial correlation matrix. However, the patch antenna array enhances the channel capacity by having a high SNR at the MT positions.

### 3.2 BS Placed at the Center of a Ceiling

In [24], we also demonstrated the enhancement of channel capacity for a BS placed at the center of a ceiling. Under this condition, the suitable radiation pattern for $4 \times 4$ MIMO systems has a HPBW of 80° and downward tilt angle of 30°, with vertical and horizontal polarizations to increase the channel capacity, as shown in Fig. 10. Ray-tracing analysis revealed that this antenna design led to an improvement of 10% in capacity compared to an isotropic antenna [24]. We also evaluated the capacity performance in a 2×2 MIMO system consisting of a small number of terminal antennas. The simulation scenarios used for the evaluation is illustrated in Fig. 11(a), and the channel capacity is shown in Fig. 11(b). In [28], we confirmed that the channel capacity for the directive radiation patterns in Fig. 10 is larger than that for dipole radiation patterns.

Based on the above-described design guidelines, we fabricated an MIMO antenna constructed using four dipole and four slot antennas (Fig. 12) [28]. In the radiation patterns of Fig. 13(a), the *xy* (horizontal) plane is the ceiling and the z-axis is in the direction (vertical plane) towards the floor. In the vertical plane, the HPBWs for the slot and dipole antennas are 84° and 85.5°, respectively. In the horizontal plane, the antenna beams are tilted, and the HPBWs in 60° from the z-axis are 61° and 53°, respectively. We conducted $2 \times 2$ MIMO channel measurements using this antenna in the scenario depicted in Fig. 14 [28]. As for the BS, the antenna is fixed to the center of the ceiling, and two streams are radiated from one slot and one dipole. The channel measurements are also conducted using sleeve arrays in the BS as the reference. Here, sleeve antennas are used for vertical and horizontal polarization. For the MT, the sleeve antenna array with elements inclined parallel and arranged perpendicular to the ground is used [28]. The channel matrices are obtained at seven room positions where no obstructions exist between the BS and MT, and all of the MT positions are in LOS. The measurement frequency is 2.45 GHz, and the detailed parameters are described in [25], [27].

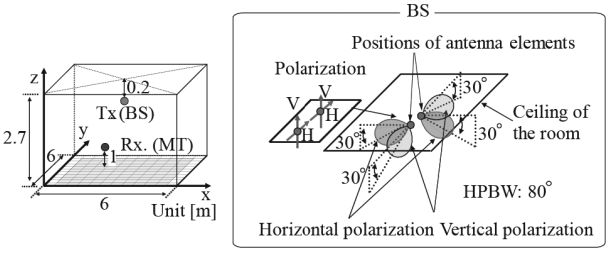


**Fig. 10** Simulation model and radiation patterns leading to large channel capacity, which are derived from ray-tracing propagation analysis.

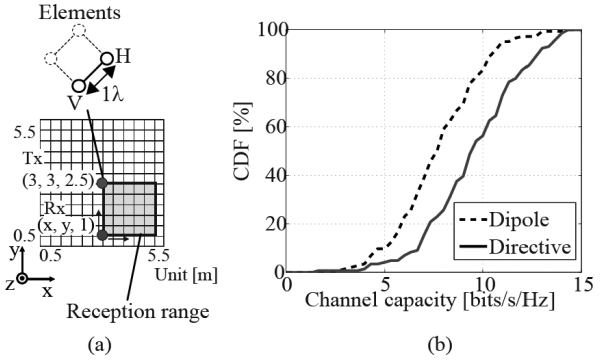


**Fig. 11** (a) Simulation scenario. (b) $2 \times 2$ MIMO capacity for the radiation patterns in Fig. 10.

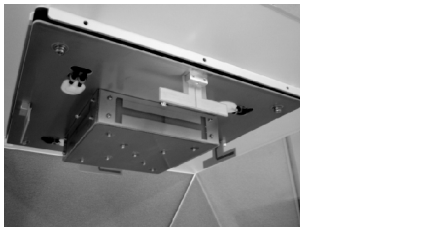

**Fig. 12** Photos of the MIMO antenna constructed using four slot and dipole antennas.

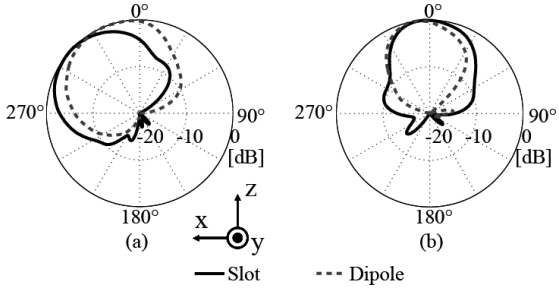


**Fig. 13** Radiation patterns for slot and dipole antenna elements in the (a) vertical plane and (b) horizontal plane tilted 30° towards the z-axis.

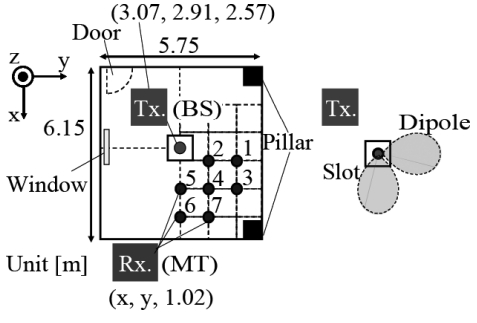


**Fig. 14** Measurement environment.

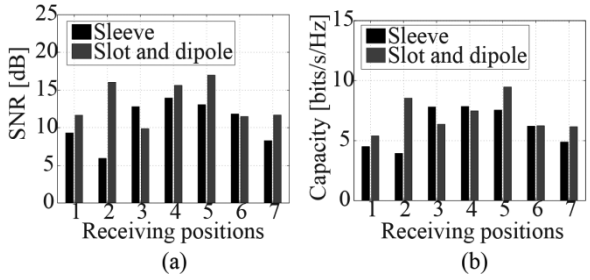


**Fig. 15** Measured (a) SNR and (b) channel capacity for the MIMO antennas constructed using either sleeve or slot and dipole antennas.

Figure 15 shows the measured SNR and channel capacities for the two antenna types. At five out of the seven examined positions, the SNR is enhanced by the slot and dipole antenna, and then the channel capacity is enhanced at four positions. The place-averaged SNR of the slot and dipole antenna is enhanced by 2.6 dB and exhibited an improvement in channel capacity of 16.2% over the sleeve antenna. A high channel capacity is obtained at positions with high SNR. Position 4 is an exception to this rule because of the degradation of the second eigenvalue, which is minimum eigenvalue, in the spatial correlation matrix. Taken together, these results indicate that directive antennas enhance not only the high-order (maximum), but also the low-order (minimum), eigenvalues in the correlation matrix.

As discussed in Sect. 2, high SNR and low spatial correlation are effective for enhancing channel capacity, which is verified by the results obtained for the directive and dual polarization antenna.

## 4. Antenna Design for MT

This section describes the mutual coupling between antennas installed in MT for enhancing the channel capacity together with the influence of radiation efficiency and pattern distortion. Mutual coupling and radiation efficiency are related to the parameters of correlation and SNR to estimate channel capacity. We also discuss the optimization of antenna radiation pattern under a realistic propagation model for MT and the effects of the head, hands, and body of users by numerical simulations with a phantom. In this section, "correlation" indicates antenna correlation since the equation of correlation assumes that distribution of incoming wave is uniform, and correlation is derived from only antenna characteristics.

### 4.1 Antenna Mutual Coupling in MT

Two major parameters, SNR and correlation, are critical to enhance channel capacity in BS antenna design. High SNR by increasing antenna gain is not easy for MT antennas, because available space in the MT is limited. The latest "smart phones" are only 55–62 mm in width, 110–126 mm in length, and 9.8–15.3 mm in thickness. Most built-in antennas are installed at the bottom of the MT to reduce the specific absorption ratio (SAR) when phones are held in the talking position. This placement location also restricts the spacing between antennas, which is necessary to obtain low correlation. For MT antennas, we focus on radiation efficiency, instead of SNR and correlation, of antenna arrays with close distance. Here, a simple simulation model based on two half wavelength dipoles is considered as an example of MT antennas, and the effects of the chassis and human body on MT antennas is discussed in Sect. 4.2.

The effects of array spacing on MIMO channel capacity were examined for an array with/without mutual coupling [29], [30]. Spatial correlation by an array factor under random incoming waves at the MT is given as,

$$\gamma_p(d) = |J_0(kd)|^2 \tag{8}$$

where $k$ is the vacuum wave number, $J_0$ is the 0th order Bessel function, and d is the spacing of the two-element array. A reduction in the correlation due to mutual coupling is advantageous for small built-in antennas, however, a drawback is small radiation efficiency. To determine the relationship between correlation and efficiency, two half wavelength dipole antennas are used in this simulation, where two dipoles are parallel in the z-axis direction and the center of one dipole is at the origin and the other dipole center is on the $x$ axis at position $x = d$. The correlation between the two dipoles is given by the scattering parameters as [31],

$$\gamma_d = \frac{\left|S_{11}^* S_{12} + S_{12}^* S_{22}\right|^2}{\left(1 - |S_{11}|^2 - |S_{21}|^2\right)\left(1 - |S_{12}|^2 - |S_{22}|^2\right)} \tag{9}$$

Assuming no losses in antenna elements, the radiation efficiency of antenna 1 is given by $S_{11}$ and $S_{21}$.

$$\eta_r = 1 - |S_{11}|^2 - |S_{21}|^2 \tag{10}$$

Mutual coupling also causes a distortion in the radiation pattern, which is defined by the ratio between the maximum and minimum gains in the $xy$ ($E$) plane as $\Delta_g = G_{max}/G_{min}$.

The evaluation factors for array spacing are shown in Fig. 16. The correlation of $\gamma_d$ is decreased by mutual coupling, which is also explained by the observed pattern distortion at values greater than 3 dB in the $xy$ plane. It should be noted that the efficiency, $\eta_r$, is decreased by small array spacing. The reduction of efficiency reduces the channel capacity. As discussed in Sect. 2, the channel capacity is approximated by Eq. (3). In the case of $2 \times 2$ MIMO systems, the ergodic channel capacity is approximated by the first term of Eq. (3) in high SNR regime. Thus, the channel capacity, including the efficiency, is approximated as

$$C(\eta) \approx N_r \log_2\left(\eta_r \frac{\rho}{N_t}\right) \tag{11}$$

The channel capacity normalized by $\eta_r$=1, as shown in Fig. 17, is reduced by small efficiency. In small-spacing arrays, the radiation efficiency should be carefully considered in the design of MT antennas [32]. The saturation in capacity increase for $\eta_r < 0.5$ in Fig. 2(b) and the discussion

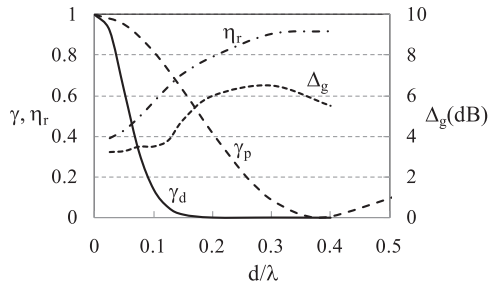


**Fig. 16** Correlation, radiation efficiency, and pattern distortion of two-element dipole antennas.

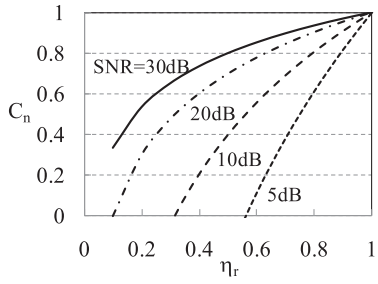


**Fig. 17** Normalized channel capacity as a function of radiation efficiency.

about efficiency result in that high radiation efficiency is a key paramter for MT antenna design.

### 4.2 Effect of the Human Body in MT Antenna Design

The preceding discussions did not consider the direction of incoming waves and the effects of chassis and human body. As these factors can dramatically alter the radiation pattern of MT antennas, the direction of incoming waves should be included to more accurately evaluate channel capacity. The results shown in Fig. 3 indicate that small spatial correlation of channels does not improve the channel capacity in Rician distributions; however, we demonstrate here that MT antennas with low correlation display channel capacity enhancement under Rician propagation environment. A propagation model that includes the direction of incoming waves is given by a model that assumes Kronecker scattering [33], where the scattering waves are not correlated with the incoming waves. A correlated scattered-wave model and a model of incoming wave with angular spread are other models for MIMO channel capacity estimation [34], however, these models reduce the absolute value of capacity and do not depend on the radiation pattern of MT antennas [35]. Thus, in the following discussion, we use only the Kronecker model.

An array of pairs of folded inverted-F antennas (IFA) mounted on a chassis top is used in the following simulation [36]. This array is introduced to determine the suitable radiation pattern for a MT. The antenna parameters are shown in Fig. 18. The array element consists of two identical IFAs with close spacing, which are connected through a phase shifter with a phase difference of $\delta$. The phase difference is

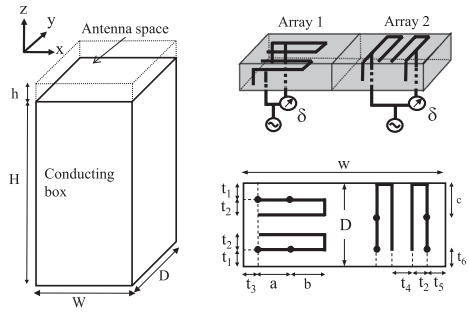


**Fig. 18** Geometry of the MT antenna. $H$=110, $W$=50, $D$=20, $h$=7, $d$=10, $a$=8, $b$=3, $c$=7, $t_1$=3, $t_2$=5, $t_3$=1, $t_4$=2.9, $t_5$=3, and $t_6$=2 (mm).

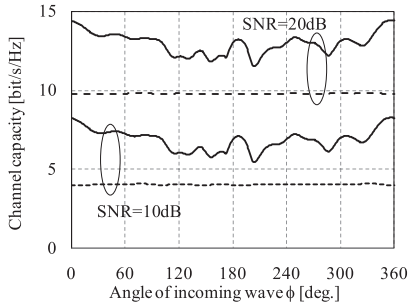


**Fig. 19** Channel capacity as a function of incoming wave direction. The solid line is $\delta$=150° and the dotted line is $\delta$=0°.

adjusted to minimize the correlation between arrays 1 and 2. The correlation is calculated based on a complex radiation pattern.

In the propagation model, the number of transmission antennas is 2, and no correlation exists between the transmission antennas. The SNRs are 10 and 20 dB, the XPR is 0 dB, and the Rician factor is 3 dB. The details of the channel capacity estimation under the conditions of this propagation model are described in [34]. For simplicity, we assume that all incoming waves are concentrated in the $xy$ plane, and the angle of incoming waves is given by $\phi$.

Figure 19 shows the channel capacity of the MT MIMO antenna with and without a phase difference between the array elements. The MT is held by the left hand of a phantom, as shown in Fig. 20. The characteristics of this model are calculated by FEKO [37]. The channel capacity with suitable phase difference is larger than that without phase difference for all examined angles of incoming waves. The average improvement factor in channel capacity is 33% for a SNR of 20 dB and 68% for a SNR of 10 dB, using a phase difference of $\delta$=150°. As described in Sect. 2, the improvement factor of the channel capacity is high in low SNR regimes, which is also verified in Fig. 19. The radiation patterns in the $xy$ plane for $\delta$=150° are shown in Fig. 21. The vertical polarization patterns are almost orthogonal, which reduces the correlation. For MT antennas, ideally, the antenna should be designed to achieve a small correlation between the antenna elements.

In practical antenna design, pattern optimization in the presence of a human body is a time-consuming step, and

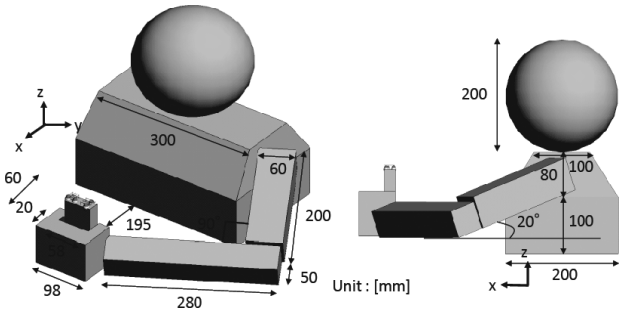


**Fig. 20** Phantom model for viewer mode. All units are in mm. Head part ($\varepsilon_r$=40, $\sigma$=1.4 S/m); other parts ($\varepsilon_r$=54, $\sigma$=1.45 S/m).

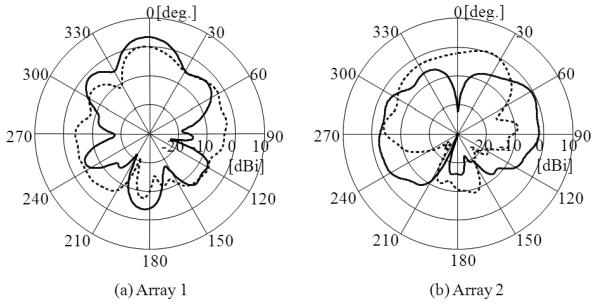


**Fig. 21** Radiation pattern of antenna in viewer mode. The solid and dotted lines are vertical and horizontal polarizations, respectively.

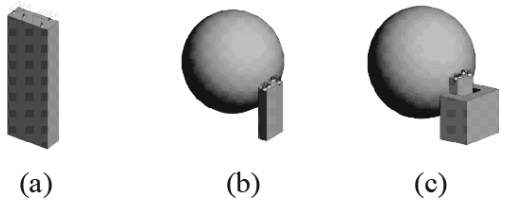


**Fig. 22** Three models for evaluating pattern optimization in a MT antenna design. (a) MT in free space, (b) MT in the talk position with head, and (c) MT in the talk position with head and hand.

is markedly more difficult than considering only a MT. We also evaluate the channel capacity of a MT for three cases (Fig. 22), which consisted of a MT in free space, a MT with a head, and a MT with a head and hand. For the three conditions, the channel capacities are enhanced by the identical phase difference of $\delta = 150°$, and the average increases are 27%, 26%, and 36%, respectively, for a SNR of 20 dB. This analysis indicates that the antenna design in free space also provides the channel capacity enhancement in the presence of a human body. Although various types of antenna designs should be evaluated by realistic phantom modeling to simulate the human body, the optimization of antenna parameters can be performed in free space.

## 5. Conclusion

This paper has evaluated two dominant design parameters, SNR and correlation, for enhancing channel capacity in MIMO systems. In the propagation channel, high SNR and low spatial correlation are necessary to enhance channel capacity, which has been described by simple formulas. We determined the suitable antenna design under indoor propagation models. The antennas characterized by HPBW and tilted beam angles were presented by a patch antenna installed at the ceiling edge and a dipole and slot antenna located at the ceiling center. The enhancement of channel capacity was verified by indoor propagation measurements.

In the design of MT antennas, we demonstrated that the radiation efficiency and mutual coupling, which are derived by a two-dipole array, have an impact on correlation and SNR, and therefore channel capacity. The mutual coupling or correlation between antennas in a MT was properly-adjusted under a Rician propagation model. The channel capacity enhancement was also verified for a MT antenna in the presence of a phantom. Notably, a suitable antenna design in free space was also effective for the design of an antenna held by hand in front of a body phantom.

## Acknowledgments

The authors thank Dr. Keizo Cho, NTT Docomo, Inc., for his useful discussion and support in the measurements.

### References

[1] A.J. Paulraj, D.A. Gore, R.U. Nabar, and H. Bölcskei, "An overview of MIMO communications — A key to gigabit wireless," Proc. IEEE, vol.92, no.2, pp.198–218, Feb. 2004.
[2] J.W. Wallace, M.A. Jensen, A.L. Swindlehurst, and B.D. Jeffs, "Experimental characterization of the MIMO wireless channel: Data acquisition and analysis," IEEE Trans. Wireless Commun., vol.2, pp.335–343, March 2003.
[3] K. Yu, M. Bengtsson, B. Ottersten, D. McNamara, P. Karlsson, and M. Beach, "Second order statistics of NLOS indoor MIMO channels based on 5.2 GHz measurements," Proc. IEEE Global Telecomm. Conf., vol.1, pp.156–160, Nov. 2001.
[4] G.L. Stuber, J.R. Barry, S.W. McLaughlin, Y. Li, M.A. Ingram, and T.G. Pratt, "Broadband MIMO-OFDM wireless communications," Proc. IEEE, vol.92, no.2, pp.271–294, Feb. 2004.
[5] S. Kurosaki, Y. Asai, T. Sugiyama, and M. Umehira, "A SDM-COFDM scheme employing a simple feed-forward inter-channel interference canceller for MIMO based broadband wireless LANs," IEICE Trans. Commun., vol.E86-B, no.1, pp.283–290, Jan. 2003.
[6] D. Piazza and K.R. Dandekar, "Reconfigurable antenna solution for MIMO-OFDM systems," Electron. Lett., vol.42, no.8, pp.446–447, April 2006.
[7] N. Honma, K. Nishimori, R. Kudo, Y. Takatori, and K. Okada, "Using MIMO approach to get out of many iterations in analog adaptive beamforming," Proc. IEEE Antennas Propag. Soc. Int. Symp., July 2008.
[8] T. Watanabe, H. Ohyane, N. Nakaminami, and Y Hiramoto, "Super-compact base station for femtocells," NTT DOCOMO Technical Journal, vol.10, no.2, pp.64–68, Sept. 2008.
[9] V. Chandrasekhar, J.G. Andrews, and A. Gatherer, "Femtocell networks: A survey," IEEE Commun. Mag., vol.46, no.9, pp.59–67, Sept. 2008.
[10] P. Kyritsi, D.C. Cox, R.A. Valenzuela, and P.W. Wolniansky, "Effect of antenna polarization on the capacity of a multiple element system in an indoor environment," IEEE J. Sel. Areas Commun., vol.20, no.6, pp.1227–1239, Aug. 2002.
[11] N. Honma, K. Nishimori, R. Kudo, Y. Takatori, T. Hiraguri, and M. Mizoguchi, "A stochastic approach to design MIMO antenna

with parasitic elements based on propagation characteristics," IEICE Trans. Commun., vol.E93-B, no.10, pp.2578–2585, Oct. 2010.
[12] T. Mitsui, M. Otani, C.H. Y. Eugene, K. Sakaguchi, and K. Araki, "Indoor MIMO channel measurements for evaluation of effectiveness of array antenna configurations," Proc. IEEE VTC 2003-Fall, vol.1, pp.84–88, Oct. 2003.
[13] N.K. Das, T. Inoue, T. Taniguchi, and Y. Karasawa, "An experiment on MIMO system having three orthogonal polarization diversity branches in multipath-rich environment," Proc. IEEE VTC 2004-Fall, vol.2, pp.1528–1532, Sept. 2004.
[14] C.Y. Chiu, J.B. Yan, and R.D. Murch, "24-port and 36-port antenna cubes suitable for MIMO wireless communications," IEEE Trans. Antennas Propag., vol.56, no.4, pp.1170–1176, April 2008.
[15] A.D. Capobianco, F.M. Pigozzo, S. Boscolo, M. Midrio, F. Sacchetto, A. Assalini, L. Brunetta, N. Zambon, and S. Pupolin, "A novel compact MIMO array based on planar Yagi antennas for multipath fading channels," Proc. 3rd European Wireless Tech. Conf., pp.95–96, Sept. 2010.
[16] L. Ndikumasabo, "MIMO antenna configuration for femtocell application," Proc. 2009 Loughborough Antennas & Propagation Conf., pp.125–128, Nov. 2009.
[17] N. Razavi-Ghods, M. Abdalla, and S. Salous, "Characterisation of MIMO propagation channels using directional antenna arrays," Proc. IEE International Conference on 3G Mobile Communication Technologies, pp.163–167, 2004.
[18] C. Hermosilla, R. Feick, R.A. Valenzuela, and L. Ahumada, "Improving MIMO capacity with directive antennas for outdoor-indoor scenarios," IEEE Trans. Wireless Commun., vol.8, no.5, pp.2177–2181, May 2009.
[19] G.J. Foschini, "Layered space-time architecture for wireless communication in fading environment using multi-element antennas," Bell Labs Tech. J., pp.41–59, Autumn 1996.
[20] D.P. McNamara, M.A. Beach, P.N. Fletcher, and P. Karlsson, "Capacity variation of indoor multiple-input multiple-output channels," Electron. Lett., vol.36, pp.2037–2038, Nov. 2000.
[21] K. Sakaguchi, H.Y.E. Chua, and K. Araki, "MIMO channel capacity in an indoor line-of-sight (LOS) environment," IEICE Trans. Commun., vol.E88-B, no.7, pp.3010–3019, July 2005.
[22] A. Paulraj, R. Nabar, and D. Gore, Introduction to space time wireless communications, Cambridge University Press, 2003.
[23] D. Uchida, T. Michihata, H. Arai, Y. Inoue, K. Cho, and T. Maruyama, "Optimum beam direction and width for directional antenna indoor MIMO systems," Proc. Int. Symp. Antennas Propag., 1D5-2, pp.165–168, Aug. 2007.
[24] D. Uchida, T. Michihata, H. Arai, Y. Inoue, and K. Cho, "Channel capacity enhancement by polarization and pattern of access point antenna in indoor MIMO systems," Proc. IEEE Antennas Propag. Soc. Int. Symp., July 2008.
[25] D. Uchida, H. Arai, Y. Inoue, and K. Cho, "Experimental assessment of the channel capacity in indoor MIMO systems using dual-polarization," Proc. IEEE VTC 2009-Spring, April 2009.
[26] D. Uchida, H. Arai, Y. Inoue, and K. Cho, "Optimum conditions in indoor MIMO systems using directional antennas at the access point," IEICE Technical Report, A·P2008-122, Nov. 2008 (in Japanese).
[27] Y. Inoue, N. Ito, and H. Arai, "$4 \times 4$ MIMO prototype system and measurement of indoor environment," Proc. 2005 Int. Symp. on Antennas Propag., WA3-4, pp.59–62, Aug. 2005.
[28] D. Uchida, H. Arai, Y. Inoue, and K. Cho, "A low-profile dual-polarized directional antenna for enhancing channel capacity in indoor MIMO systems," IEICE Trans. Commun., vol.E93-B, no.10, pp.2570–2577, Oct. 2010.
[29] T. Ohgane, "Base and element technology of MIMO system," IEICE Workshop, no.29, 2004 (in Japanese).
[30] H. Iura, H. Yamada, Y. Ogawa, and Y. Yamaguchi, "Effect of array spacing on MIMO channel capacity," IEICE Technical Report, A·P2004-69, July 2004 (in Japanese).
[31] J. Thaysen and K.B. Jakobsen, "Envelope correlation in (N,N) MIMO antenna array from scattering parameters," Microwave and Optical Technology Letters, vol.48, no.5, May 2006.
[32] H. Sato, Y. Koyanagi, and M. Takahashi, "Study on antenna efficiency improvement of two closely monopole antenna elements," IEICE Technical Report, A·P2010-118, Dec. 2010 (in Japanese).
[33] J.P. Kermoal, L. Schumacher, K.I. Pedersen, P.E. Mogensen, and F. Frederiksen, "A stochastic MIMO radio channel model with experimental validation," IEEE J. Sel. Areas Commun., vol.20, no.6, pp.1211–1226, Aug. 2002.
[34] Y. Karasawa, "Statistical multipath propagation modeling for broadband wireless systems," IEICE Trans. Commun. (Japanese Edition), vol.E90-B, no.3, pp.468–484, March 2007.
[35] H. Arai and J. Ohno, "Channel capacity enhancement by pattern controlled handset antenna," Radioengineering, vol.18, no.4, pp.413–417, Dec. 2009.
[36] D. Uchida, J. Ohno, and H. Arai, "Capacity enhancement using fixed phase difference feeding in a handset MIMO antenna including human body effects," International Conference on Applications of Electromagnetism and Student Innovation Competition Awards (AEM2C 2010), Taipei, Taiwan, Aug. 11-13, 2010.
[37] http://www.feko.info/

**Hiroyuki Arai** received the B.E. degree in Electrical and Electronic Engineering, M.E. and D.E. in Physical Electronics from Tokyo Institute of Technology in 1982, 1984 and 1987, respectively. After a research associate in Tokyo Institute of technology, he joined to Yokohama National University as a lecturer in 1989. Now he is a professor in Division of Electrical and Computer Engineering, Yokohama National University. He was a visiting scholar at University of California, Los Angeles in 1997 and was visiting professor at Yonsei University, Seoul in 2005. He investigated microwave passive components for high power handling applications such as RF plasma heating in large Tokamaks. He developed a flat diversity antenna for mobile telephone terminal, a polarization diversity base station antenna for Japanese PDC systems, and small base station antennas of Inbuilding micro cellular system. His current research interest includes hardware realization of adaptive antenna system for high speed wireless data transmission. He received the Young Engineers Award from the IEICE of Japan in 1989 and the "Meritorious Award on Radio" by the Association of Radio Industries and Businesses in 1997 for the development of polarization diversity antenna and in 2006 for the development of DOA estimation system. He was serving as Secretary of Technical Group on Antennas and Propagation of IEICE from 2002 to 2004 and was editor-in-chief of IEICE Transactions on Communications from 2005 to 2007. He is currently Chair of IEEE AP-S Japan Chapter and a Fellow of the IEICE.

**Daisuke Uchida** received the B.E. and M.E. degrees in the Division of Electrical and Computer Engineering, Yokohama National University in 2007 and 2009, respectively. He is currently working toward the D.E. degree at Yokohama National University. His research interests include MIMO propagation analysis and measurement. He received the IEEE VTS Japan 2009 Young Researcher's Encouragement Award, ISAP2009 Student Paper Award in 2009 and AEM2C 2010 Best Paper Awards/The Third Prize Award in 2010. He is a student member of the IEEE.